Eur. Phys. J. Special Topics **151**, 51–57 (2007)

DOI: 10.1140/epjst/e2007-00361-x

THE EUROPEAN PHYSICAL JOURNAL SPECIAL TOPICS

Coherent backscattering of light from saturated atoms

V. Shatokhin[1,2,a], T. Wellens[3,b], C.A. Müller[4,c], and A. Buchleitner[2,d]

[1] B.I. Stepanov Institute of Physics, National Academy of Sciences, 220072 Minsk, Belarus
[2] Max-Planck-Institut für Physik komplexer Systeme, Nöthnitzer Strasse 38, 01187 Dresden, Germany
[3] Institut für Theoretische Physik, Universität Erlangen-Nürnberg, Staudstrasse 7, 91058 Erlangen, Germany
[4] Physikalisches Institut, Universität Bayreuth, 95440 Bayreuth, Germany

Abstract. We survey recent progress achieved in understanding the impact of inelastic processes on coherent backscattering of light from cold atoms that are saturated by a powerful laser field.

1 Introduction

Coherent backscattering (CBS) of light is a dazzling example of interference phenomena surviving a disorder average in multiply scattering media [1]. It occurs generally when shining light onto an optically thick, disordered sample, provided that the wave's phase coherence remains preserved over many scattering events. In this so-called "mesoscopic regime", interference effects lead to a complicated speckle pattern of the wave intensity scattered into different directions. This pattern can be seen as a fingerprint of the specific disorder realization. When averaging over the disorder, however, most of the speckles are washed out. The only interference peak non-sensitive to disorder is the one in exact backscattering direction. It originates from constructive interference between waves interacting with the same scatterers, but in opposite order, see figure 1(b). In the ideal case of perfectly constructive two-wave interference, the peak-to-background ratio of backscattered intensities, known as the enhancement factor α (see figure 1(a)), equals exactly two, whereas $\alpha < 2$ if decoherence or dephasing effects are present.

CBS clearly shows that, in general, wave propagation in disordered media cannot be fully described by a simple diffusion equation. In the case of weak disorder, an approximate diffusion model can nevertheless be maintained, provided that the enhanced backscattering effect is accounted for by a reduction of the diffusion constant (weak localization). For strong disorder, i.e., if the mean free path becomes comparable to the wave length, interference between reversed paths can even lead to a complete absence of diffusion (strong localization) [2]. A promising candidate for reaching the strong disorder regime experimentally, is the scattering of light by cold atoms, which exhibit an extremely large resonant cross section.

Since the first experimental observation of CBS from cold atoms in 1999 [3], numerous theoretical and experimental activities have been devoted to elucidating relevant dephasing mechanisms, such as Raman scattering on the degenerate atomic transitions [4–9], the influence of a magnetic field [10,11], thermal motion of atoms [12–14], and nonlinear response of saturated

[a] e-mail: shatok@pks.mpg.de
[b] e-mail: Thomas.Wellens@physik.uni-erlangen.de
[c] e-mail: Cord.Mueller@uni-bayreuth.de
[d] e-mail: abu@pks.mpg.de

dipole transitions [15–22]. Experiments have been performed on two atomic species, rubidium (Rb) [3,8,12,13,16] and strontium (Sr) [15,23].

In the present mini-review, we focus on the impact of inelastic scattering from strongly driven, saturated atomic dipole transitions on CBS. Understanding this dephasing mechanism, induced by quantum mechanical frequency fluctuations of the scattered photons, is important for the transition from weak to strong localization, which is expected to occur at increased atomic densities, when atoms exchange multiple photons, and even a single photon is able to saturate the atomic transition [15]. Apart from its fundamental interest, controlling this phase-breaking mechanism is crucial for more technological applications such as random lasers [24].

2 The model

Considering a system of only two atoms suffices to grasp the essential physical phenomena [17,18,21,22]. This relatively simple theoretical model describes an optically thin atomic medium, where double scattering provides the dominant contribution to the CBS signal [4,23]. It is in this double scattering regime that a CBS reduction due to the saturation of atomic dipole transitions was first observed [15].

Our two-atom model system is described by the Hamiltonian

$$H = H_A + H_F + H_{AF} + H_{AL}. \tag{1}$$

Here, H_A is the sum of the atomic Hamiltonians describing the electronic dipole transitions of identical, motionless atoms at random positions $\mathbf{r}_1$ and $\mathbf{r}_2$, with the distance $r = |\mathbf{r}_1 - \mathbf{r}_2|$ much greater than the optical resonance wavelength λ. The atomic internal structure corresponds to the transition $J_g = 0 \leftrightarrow J_e = 1$, precisely as in the Sr experiment [15]. The atoms are coupled to the quantized photon field bath H_F. The atom-field interaction H_{AF} leads to the radiative linewidth 2γ of the atomic excited level. This interaction also permits the two atoms to exchange resonant photons which implies a far-field dipole-dipole coupling of order $g \sim 1/kr$. Since we are considering the weak localization regime $kr \gg 1$, the small coupling $g \ll 1$ implies that atoms exchange only single photons with each other. However, the atoms are exposed to an external driving laser field with wavevector $\mathbf{k}_L$ and frequency ω_L, the coupling being described by the last term in equation (1).

Two important parameters describe the atom-laser interaction: the detuning $\delta = \omega_L - \omega_0 \ll \omega_0$ from the optical resonance at transition frequency ω_0, and the Rabi frequency Ω describing the dipole coupling strength. The effective laser intensity is conveniently described [25] by the saturation parameter $s = \Omega^2/2(\gamma^2 + \delta^2)$. If $s \ll 1$, the atoms scatter photons elastically, while $s \simeq 1$ indicates the onset of inelastic scattering, where the frequency of the scattered photons is different from the laser frequency.

3 Results

3.1 CBS intensity and enhancement factor

A quantity of primary interest is the CBS enhancement factor α measuring the phase coherence between counter-propagating waves:

$$\alpha = \frac{L_2^{\text{tot}} + C_2^{\text{tot}}}{L_2^{\text{tot}}}. \tag{2}$$

It is the total CBS intensity, measured at backscattering $\mathbf{k} = -\mathbf{k}_L$, divided by the total background intensity L_2^{tot} measured away from the backward direction, the index "2" indicating the double scattering contribution. The radiated field amplitude is proportional to the electric

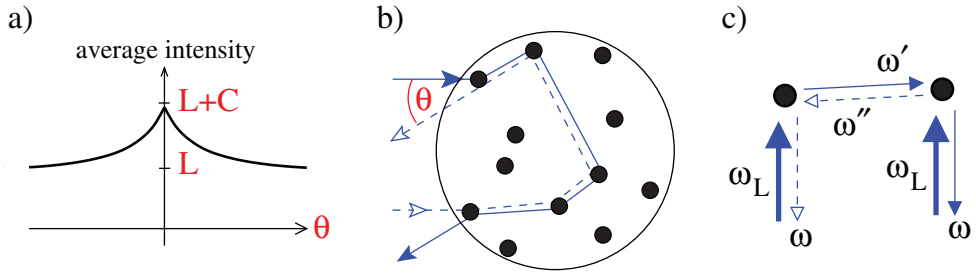

Fig. 1. a), b) General mechanism of coherent backscattering: constructive interference between waves travelling along reversed scattering paths leads to an enhancement of the average intensity scattered from a disordered sample in backwards direction $\theta = 0$. c) In this paper, we examine the fundamental case of two strongly laser driven atoms. Frequency fluctuations due to inelastic scattering break the symmetry between the reversed paths ($\omega' \neq \omega''$), leading to dephasing and reduction of the coherent backscattering peak.

dipole of the emitting atom [25]. The scattered intensities, i.e., background $L_2^{\rm tot}$ and interference $C_2^{\rm tot}$ contributions, can therefore be expressed via certain dipole correlation functions and excited state populations, respectively, of the two atomic CBS transition.

Figure 1(c) shows one example of the nonlinear inelastic scattering processes, induced by a powerful laser field, contributing to the CBS interference $C_2^{\rm tot}$. Note that the intermediate photon frequencies of the counter-propagating processes are, in general, different from each other, leading to the violation of the reciprocity symmetry between the reversed paths, and hence to a decrease of α.

Starting from the Hamiltonian (1), we have derived [18,21] the two-atom master equation governing the evolution of arbitrary two-atom observables. Thus, CBS intensities and, hence, the enhancement factor can be found by solving the master equations and performing a configuration average of the results over the probability distributions of $\mathbf{r}_1$ and $\mathbf{r}_2$. In many cases, analytical solutions are found, while general results are accessible from numerical solutions. In the following, we will report results for the helicity preserving polarization channel, referring the interested reader to [21] for more general cases.

Both $C_2^{\rm tot}$ and $L_2^{\rm tot}$ can be decomposed into elastic and inelastic components, $C_2^{\rm tot} = C_2^{\rm el} + C_2^{\rm inel}$, $L_2^{\rm tot} = L_2^{\rm el} + L_2^{\rm inel}$. Figure 2 shows the elastic parts $L_2^{\rm el} = C_2^{\rm el}$ (the equality holds thanks to reciprocity), the inelastic background $L_2^{\rm inel}$ and interference term $C_2^{\rm inel}$ (right y axis), as well as the enhancement factor α (left y axis), all as function of the saturation s for two different detunings: (a) on-resonance $\delta = 0$ and (b) $\delta = 20\gamma$.

The on-resonance enhancement factor in figure 2(a) decreases linearly with small s, in qualitative agreement with the experiment [15].[1] In the highly saturated regime $s \gg 1$, the elastic intensity is negligible, yet the limit value $\alpha_\infty = 23/21$ larger than unity demonstrates the residual (self-)interference of inelastically scattered photons [18].

In the case of far-detuned driving shown in figure 2(b), an enhancement $\alpha < 1$ *smaller* than unity around $s \simeq 1/2$ implies the presence of CBS anti-enhancement [21], due to the destructive interference with $C_2^{\rm inel} < 0$ of the inelastic photons (cf. [12] for a similar effect in a different situation). The general condition for CBS anti-enhancement in the saturation regime can be formulated as $\Omega \simeq |\delta| \gg \gamma$, which corresponds to $s \simeq 1/2$. Also in the far-detuned case, α tends to a limit value as $s \to \infty$, which is larger than unity but smaller than α_∞.

3.2 CBS spectrum

The results shown in section 3.1 clearly demonstrate that inelastic photons do contribute to the CBS interference. It is therefore interesting to resolve the spectral characteristics of the

[1] This loss of interference visibility can be traced back to the availability of which-path information encoded in inelastically scattered photons [17]; see also the similar situation for thermal motion [14] and internal degeneracy [26].

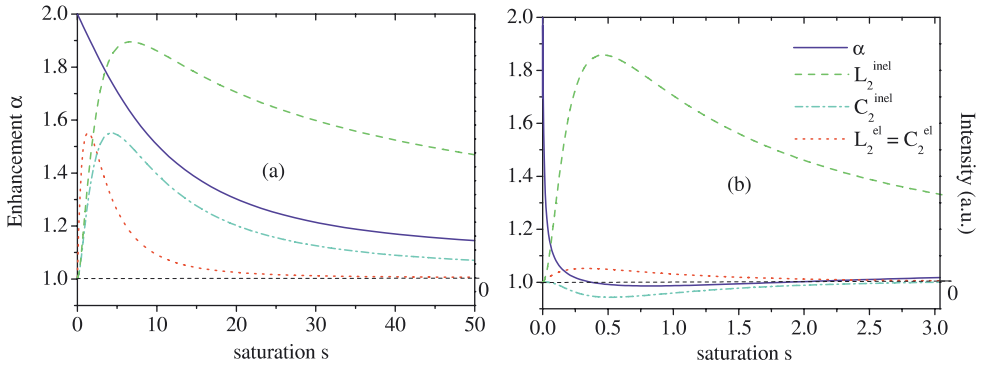

Fig. 2. Enhancement factor α (solid) vs. saturation s for (a) exact on-resonance driving ($\delta = 0$), and (b) detuned driving ($\delta = 20\gamma$). The dashed, dashed-dotted, and dotted lines represent the inelastic background $L_2^{\rm inel}$, the inelastic interference $C_2^{\rm inel}$, and the elastic $L_2^{\rm el} = C_2^{\rm el}$ intensities, respectively. The fact that α approaches a limit $\alpha_\infty = 23/21 > 1$ for $s \to \infty$ signals constructive photon (self-)interference in the deep inelastic regime.

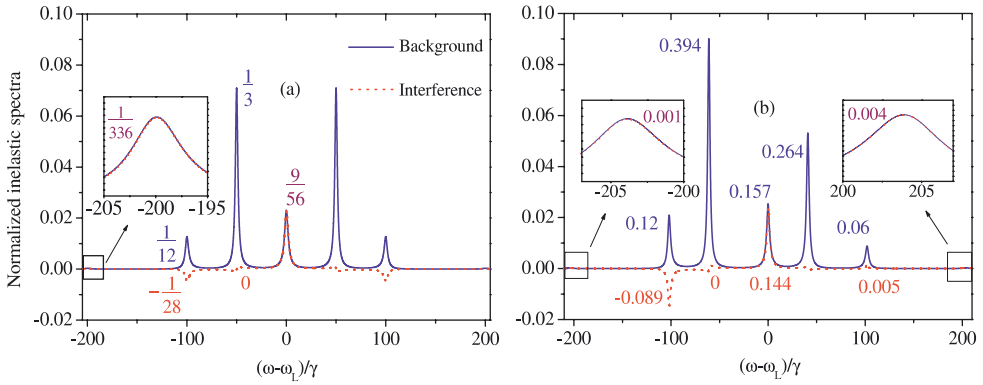

Fig. 3. Normalized inelastic spectra of the background (solid) and interference (dotted) terms, in the limit of well separated spectral lines, at $\Omega = 100\gamma$. (a) $\delta = 0$; (b) $\delta = 20\gamma$. The numbers near the resonances indicate their areas, such that the overall areas of the background and interference terms give unity and $C_2^{\rm inel}/L_2^{\rm inel}$, respectively. This corresponds to (a) $\alpha = \alpha_\infty \simeq 1.096$; (b) $\alpha = 1.065$.

background and interference contributions. In other words, instead of measuring the total intensities defining $L_2^{\rm tot}$ and $C_2^{\rm tot}$, we wish to detect the backscattered light by a narrowband detector tuned to a frequency ω. Such a set-up, completely in the spirit of figure 1(c), enables one to probe the elementary scattering processes contributing to the CBS signal at the frequency ω. By varying ω, it is possible to obtain a more detailed characterization of the inelastic processes having impact on the CBS signal in the saturation regime.

In figure 3, we present the CBS spectrum in the limit of well separated spectral lines of the single-atom resonance fluorescence spectrum ($\Omega \gg \gamma$). These results were calculated (analytically for exact on-resonance, and numerically for detuned driving) with the same master equation approach in combination with the quantum regression theorem [27,28].

In the limit $\Omega \gg \gamma$, the elastic intensity vanishes, and the CBS spectrum is purely inelastic (see figure 3). Both the background and interference spectra consist of seven resonances. The resonances of the background spectra are Lorentzians with positive weights, defining areas of the respective peaks in figure 3. As for the interference contribution, its spectrum represents a combination of the Lorentzian peaks with positive and negative weights as well as dispersive resonances. The total areas of the interference resonances, 2/21 for $\delta = 0$ and 0.065 for $\delta = 20\gamma$, allow to deduce the values of the CBS enhancement factor, $\alpha = 23/21$ and $\alpha = 1.065$, respectively.

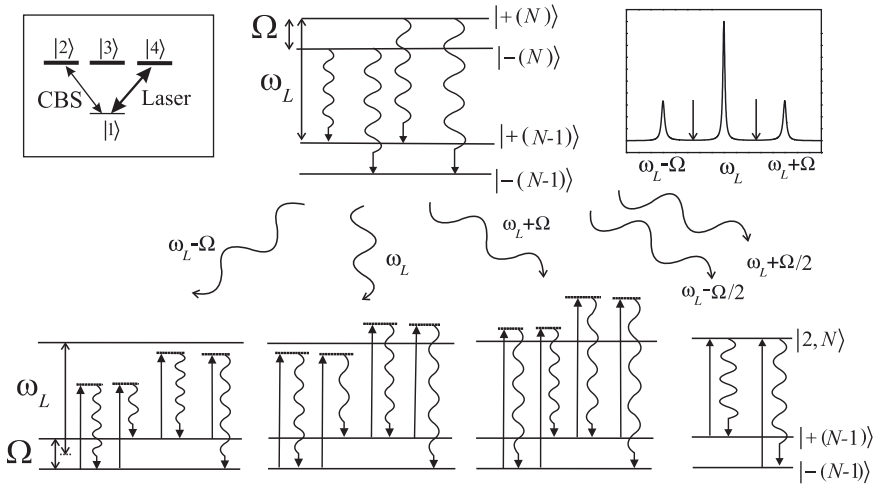

Fig. 4. Internal structure of the laser driven and CBS transitions of the atoms. Spontaneous emission processes between dressed states (top, center) give rise to the Mollow triplet (top, right) with peaks centered at $\omega_L - \Omega$, ω_L, and $\omega_L + \Omega$. Apart from these, one needs to take into account photons with frequencies $\omega_L \pm \Omega/2$, indicated by the two downward arrows in the plot of the Mollow triplet. The photons emitted by atom 1 (wiggly arrows with indicated frequencies) propagate to atom 2 (bottom), where they are (re-)scattered from either of the dressed states $|+(N-1)\rangle$, $|-(N-1)\rangle$, finally giving rise to seven different peaks in the two-atom spectrum (figure 3).

The number and positions of the CBS spectral peaks can be understood within a dressed-state analysis of the atomic laser-driven and CBS transitions (see figure 4)[2]. We assume a right circular polarization of the laser field driving the $|1\rangle \leftrightarrow |4\rangle$ transition of both atoms. Then, observing CBS in the helicity preserving channel corresponds to detecting photons emitted from the $|1\rangle \leftrightarrow |2\rangle$ (figure 4, top left).

The interaction of the atoms with the powerful laser field leads to the formation of dressed states [25]

$$|\pm(N)\rangle = 2^{-1/2}(|1, N+1\rangle \pm |4, N\rangle), \tag{3}$$

where N is the number of photons in the laser mode (figure 4, top center). Spontaneous transitions from the dressed-state manifold $\{|\pm(N)\rangle\}$ to $\{|\pm(N-1)\rangle\}$ give a resonance fluorescence spectrum with three peaks centered at $\omega_L - \Omega$, ω_L, and $\omega_L + \Omega$, which is known as the Mollow triplet [29] (figure 4, top right). Photons emitted by one atom are re-scattered on the CBS transition of the other atom. The level $|2\rangle$ of the latter transition is not affected by the laser laser field. However, the $|1\rangle \leftrightarrow |2\rangle$ transition is modified by the laser field, because it shares the common level $|1\rangle$ with the laser-driven transition. Therefore, the internal structure of the CBS transition is such as shown in figure 4(bottom): it has one excited state and two ground state sublevels separated by Ω. Correspondingly, the new resonance frequencies of the CBS transition are $\omega_L \pm \Omega/2$.

When the Mollow triplet emitted by one atom is incident on another atom, it is scattered on the internal structure of the latter. The relevant scattering processes that can take place are depicted on the bottom of figure 4. Each photon can be scattered either elastically or undergo Raman-Stokes or anti-Stokes (multiphoton) transitions (which lead to a frequency change by $-\Omega$ or Ω, respectively), which conserve energy and angular momentum. It follows that the CBS spectrum must have resonances at $\omega = \omega_L \pm 2\Omega$, $\omega = \omega_L \pm \Omega$, and $\omega = \omega_L$. The diagrams describing the emission of CBS photons at these frequencies are the three left-most diagrams on the bottom of figure 4. The right-most diagram in figure 4(bottom) depicts resonant scattering of photons with frequencies $\omega_L \pm \Omega/2$, which leads to an additional doublet – the Autler-Townes doublet [30] – in the CBS spectrum.

[2] This figure corresponds to $\delta = 0$, but remains qualitatively the same for $\delta \neq 0$.

The above analysis can straightforwardly be extended to the general case $\delta \neq 0$. Again, the background and interference spectra both consist of seven resonances (see figure 3(b)) which represent: (i) a (re-)scattered Mollow triplet [29] at $\omega = \omega_L$, $\omega_L \pm \Omega'$, where $\Omega' = (\Omega^2 + \delta^2)^{1/2}$, (ii) an Autler-Townes doublet [30] at $\omega = \omega_L \pm (\Omega' \mp \delta)/2$, and (iii) a doublet at $\omega = \omega_L \pm 2\Omega'$ originating from Raman-Stokes and anti-Stokes scattering of the Mollow triplet sidebands .

Whether the interference of amplitudes at a certain frequency is constructive or destructive is determined by their relative frequency-dependent phase shifts [28]. The interference is purely constructive around $\omega = \omega_L$ and $\omega = \pm 2\Omega'$, whereas it changes its character around the dispersive resonance peaks of the Autler-Townes doublet. Finally, the interference can be destructive for one or both of the Mollow sidebands (see figure 3). At $|\delta| \simeq \Omega$, these destructive interferences can outweigh the constructive ones in the sum over all spectral contributions, resulting in CBS anti-enhancement for the total intensity.

4 Conclusion and outlook

We have studied the impact of inelastic processes on CBS within a simple quantum optical model involving two atoms exposed to a strong laser field. Within our master-equation approach, we can calculate the loss of CBS interference for all values of saturation and detuning, including an analysis of the spectral components. A dressed-state picture permits to understand the position and character of resonance peaks that constitute the background and interference signals.

Including higher scattering orders as well as addressing propagation effects in bulk atomic clouds is hard within this framework, due to the exponential growth of the Hilbert space with the number of scatterers. A promising direction of future research is to unify the presently discussed master-equation description of atom-photon interaction with the diagrammatic scattering approach that has been developed for nonlinear classical scatterers [19,20]. Further challenging problems include a quantitative explanation of the CBS experiment in the saturation regime with internally degenerate Rb atoms [16], the assessment of quantum statistical properties of the backscattered field, and, ultimately, the exploration of the strong localization regime $kr \simeq 1$.

References

1. E. Akkermans, G. Montambaux, J.-L. Pichard, J. Zinn-Justin (eds.), *Mesoscopic Quantum Physics* (Elsevier, Amsterdam, 1994)
2. D. Vollhardt, P. Wölfle, Phys. Rev. B **22**, 4666 (1980)
3. G. Labeyrie et al., Phys. Rev. Lett. **83**, 5266 (1999)
4. T. Jonckheere et al., Phys. Rev. Lett. **85**, 4269 (2000)
5. C.A. Müller, T. Jonckheere, C. Miniatura, D. Delande, Phys. Rev. A **64**, 053804 (2001)
6. C.A. Müller, C. Miniatura, J. Phys. A **35**, 10163 (2002)
7. D.V. Kupriyanov et al., Phys. Rev. A **67**, 013814 (2003)
8. G. Labeyrie, D. Delande, C.A. Müller, C. Miniatura, R. Kaiser, Europhys. Lett. **61**, 327 (2003)
9. C.A. Müller, C. Miniatura, D. Wilkowski, R. Kaiser, D. Delande, Phys. Rev. A **72**, 053405 (2005)
10. G. Labeyrie et al., Phys. Rev. Lett. **89**, 163901 (2002)
11. O. Sigwarth et al., Phys. Rev. Lett. **93**, 143906 (2004)
12. D.V. Kupriyanov et al., Phys. Rev. A **69**, 033801 (2004)
13. G. Labeyrie, D. Delande, R. Kaiser, C. Miniatura, Phys. Rev. Lett. **69**, 013004 (2006)
14. C. Wickles, C.A. Müller, Europhys. Lett. **74**, 240 (2006)
15. T. Chanelière, D. Wilkowski, Y. Bidel, R. Kaiser, C. Miniatura, Phys. Rev. E **70**, 036602 (2004)
16. S. Balik et al., J. Mod. Opt. **52**, 2269 (2005)
17. T. Wellens, B. Grémaud, D. Delande, C. Miniatura, Phys. Rev. A **70**, 023817 (2004)
18. V. Shatokhin, C.A. Müller, A. Buchleitner, Phys. Rev. Lett. **94**, 043603 (2005)
19. T. Wellens, B. Grémaud, D. Delande, C. Miniatura, Phys. Rev. E **71**, 055603(R) (2005)
20. T. Wellens, B. Grémaud, D. Delande, C. Miniatura, Phys. Rev. A **73**, 013802 (2006)
21. V. Shatokhin, C.A. Müller, A. Buchleitner, Phys. Rev. A **73**, 063813 (2006)
22. B. Grémaud, T. Wellens, D. Delande, C. Miniatura, Phys. Rev. A **74**, 033808 (2006)

23. Y. Bidel et al., Phys. Rev. Lett. **88**, 203902 (2002)
24. H. Cao, Waves Random Media **13**, R1 (2003)
25. C. Cohen-Tannoudji, J. Dupont-Roc, G. Grynberg, *Atom-Photon Interactions* (Wiley, New York, 1992)
26. C. Miniatura, C.A. Müller, Y. Lu, G. Wang, B.-G. Englert, arXiv:0704.1896 (accepted in Phys. Rev. A)
27. V. Shatokhin, Opt. Spectrosc. **103**, 281 (2007); arXiv:quant-ph/0608094 (2006)
28. V. Shatokhin, T. Wellens, B. Grémaud, A. Buchleitner (submitted)
29. B.R. Mollow, Phys. Rev. **188**, 1969 (1969)
30. S.H. Autler, C.H. Townes, Phys. Rev. **100**, 703 (1955)